Water Research 162 (2019) 518–527

Contents lists available at ScienceDirect

Water Research

journal homepage: www.elsevier.com/locate/watres

Diffusion of hydrophilic organic micropollutants in granular activated carbon with different pore sizes

Laura Piai [a], Jouke E. Dykstra [a], Mahesa G. Adishakti [a, 1], Marco Blokland [b], Alette A.M. Langenhoff [a, *], Albert van der Wal [a, c]

[a] Environmental Technology, Wageningen University & Research, P.O. Box 17, 6700 AA Wageningen, The Netherlands
[b] Wageningen Food Safety Research, Wageningen University & Research, P.O. Box 230, 6708 WB Wageningen, The Netherlands
[c] Evides Water Company, P.O. Box 4472, 3006 AL, Rotterdam, The Netherlands

ARTICLE INFO

Article history:
Received 14 February 2019
Received in revised form
9 May 2019
Accepted 5 June 2019
Available online 6 June 2019

Keywords:
Hydrophilic micropollutants
Activated carbon
Adsorption kinetics
Intra-particle diffusion
Pore diffusion

ABSTRACT

Hydrophilic organic micropollutants are commonly detected in source water used for drinking water production. Effective technologies to remove these micropollutants from water include adsorption onto granular activated carbon in fixed-bed filters. The rate-determining step in adsorption using activated carbon is usually the adsorbate diffusion inside the porous adsorbent. The presence of mesopores can facilitate diffusion, resulting in higher adsorption rates. We used two different types of granular activated carbon, with and without mesopores, to study the adsorption rate of hydrophilic micropollutants. Furthermore, equilibrium studies were performed to determine the affinity of the selected micropollutants for the activated carbons. A pore diffusion model was applied to the kinetic data to obtain pore diffusion coefficients. We observed that the adsorption rate is influenced by the molecular size of the micropollutant as well as the granular activated carbon pore size.

1. Introduction

Anthropogenic organic micropollutants (OMPs), like pharmaceuticals, industrial chemicals, pesticides, and their transformation products, are often found in surface and groundwater (Christoffels et al., 2016; Loos et al., 2010; Ruff et al., 2015; Scheurer et al., 2009). OMPs may enter the environment via the effluent of wastewater treatment plants and runoff from agricultural land. In the past decades, dozens of OMPs have been detected in water bodies used for drinking water production (Sjerps et al., 2016; ter Laak et al., 2014). Amongst other reasons, this is related to the advance of analytical techniques, which have become more sensitive and selective (Reemtsma et al., 2016a; Ternes, 2007). Due to increasing use of anthropogenic organic chemicals, the contamination of surface and drinking water with OMPs will likely increase in the future.

Polar OMPs are less efficiently removed in wastewater treatment plants as well as in drinking water treatment plants (Reemtsma et al., 2016b). Screening studies have revealed a relative increase in polar compounds in drinking water samples compared to composition in surface or groundwater (Sjerps et al., 2016). It is often found that the concentration of OMPs in drinking water exceeds 1 μg/L (RIWA-Maas, 2016), which indicates the need for improving current drinking water treatment technologies.

Adsorption onto activated carbon (AC) in fixed-bed filters is one of the main steps for OMP removal during drinking water production from surface water sources (Stackelberg et al., 2007; Ternes, 2007; Ternes et al., 2002). Although, activated carbon is known to be more effective for adsorption of hydrophobic compounds, removal of hydrophilic compounds has been also reported (Nam et al., 2014; Nguyen et al., 2012). Technologies involving adsorption onto AC are cost-effective and normally no transformation products are formed, in contrast to advanced oxidation processes (Gunten, 2018; Miklos et al., 2018). Drawbacks of AC adsorption technologies include the high energy consumption for AC regeneration and slow adsorption kinetics (Worch, 2012). Nevertheless, adsorption onto activated carbon is still regarded as an effective step to remove OMPs from wastewater and drinking water (Katsigiannis et al., 2015).

Activated carbon is a versatile adsorbent due to its affinity for a wide range of compounds and large internal surface area (Nath and

* Corresponding author.
E-mail address: alette.langenhoff@wur.nl (A.A.M. Langenhoff).
[1] Environmental Resources Management Indonesia, Centennial Tower, South Jakarta, 15419, Indonesia.

https://doi.org/10.1016/j.watres.2019.06.012

Bhakhar, 2011; Worch, 2012). The large surface area of AC originates from the complex internal porous structure, formed during the activation process. To reach the internal surface area where adsorption takes place, the OMPs must diffuse from the solution into the pores. We can distinguish three different compartments in which transport takes place: 1) the bulk solution, 2) the thin film layer around the AC particle, and 3) the inside of the particle. The transport in the intra-particle compartment is due to surface and pore diffusion. In surface diffusion, the OMP that is adsorbed onto the AC surface is transported along the carbon internal surface, whereas in pore diffusion the OMP is transported in the liquid phase within the carbon pores. Adsorption kinetics are determined by film, surface and/or pore diffusion, although the relative contributions are dependent on such parameters as mixing regime, adsorbent type and adsorbate properties. It is important to note that in practice it is often difficult to distinguish between surface and pore diffusion (Valderrama et al., 2008).

The rate limiting step during adsorption of OMPs onto AC can be identified through modelling approaches accounting for the properties of both adsorbate and adsorbent. Lower diffusion rates reduce the efficiency of AC filters due to a more dissipated area between loaded and unloaded zones in the filter bed. Consequently the adsorbate is found in the effluent before the filter bed has been used to its maximum adsorption capacity (Worch, 2012). By modelling the adsorption kinetics of different OMPs onto activated carbon, the apparent diffusion coefficient of the micropollutant in activated carbon can be obtained. This information can then be used to model and optimize removal of OMPs in AC filters.

In this study we assess the affinity of hydrophilic OMPs for two different types of granular activated carbon (GAC) with different pore structure and develop a theoretical model, based on pore diffusion, to describe the adsorption kinetics. Adsorption isotherms and kinetic experiments were used as input for the model to obtain apparent pore diffusion coefficients of 9 OMPs of different sizes using 2 GACs with different pore sizes. The results provide insight in which of the characteristics of OMPs and ACs affect the adsorption rate.

2. Diffusion model

Several models have been presented in literature to describe adsorption kinetics in porous adsorbents. Some models assume that the transport rate is determined by the adsorption of the adsorbate onto the adsorbent surface. They describe the adsorption rate as a chemical reaction (Ocampo-Pérez et al., 2015). Examples of models using this approach are pseudo-first-order and pseudo-second-order kinetic models as described by Ho and McKay (1998) and Blanchard et al. (1984). Such models usually fit the data well, but have limited predictive value since the parameters have no physical meaning (Lesage et al., 2010). On the other hand, some models assume that the adsorption rate is determined by diffusion. Those are more realistic models based on parameters that are related to the physical and chemical properties of the adsorbent, such as adsorbent porosity and particle radius (Kyriakopoulos and Doulia, 2006). These models take into account film diffusion and/or intra-particle diffusion (Hung and Lin, 2006; Lee and Mckay, 2004; Valderrama et al., 2008).

Intra-particle diffusion can be modelled based on surface and/or pore diffusion, depending on which process determines the rate in the system studied. In some studies pore diffusion is described as the dominant transport mechanism (Ocampo-Pérez et al., 2012b), others find a greater contribution from surface diffusion (Ocampo-Perez et al., 2011, 2010; Zhu et al., 2016), or conclude that both transport processes are relevant (Souza et al., 2017). In general, it is difficult to distinguish between surface and pore diffusion in practice. There are no known properties of the adsorbate and the GAC, nor known conditions of the adsorption process that determine the dominant transport mechanism. Ocampo-Pérez et al. (2015) found that low adsorption capacity of the carbon towards an adsorbate resulted in a higher relative contribution of pore diffusion to the intraparticle diffusion. We assume that pore diffusion will be a relevant diffusion mechanism of hydrophilic compounds in GAC given their lower affinity in comparison to hydrophobic compounds.

We used a pore diffusion model (PDM) to describe the mass transfer of micropollutants towards the internal surface of activated carbon. All OMPs studied in our experiments are hydrophilic, which have in general a lower affinity for AC than hydrophobic micropollutants. Pore diffusion, therefore, was expected to be the dominant mass transfer mechanism. In the model, we consider only pore diffusion for the mass transfer inside the pores. Comparable models have been reported in literature (Ocampo-Pérez et al., 2012a, 2012b; Souza et al., 2017). In the PDM, the AC granules are assumed to be spherical with a constant diameter and homogeneous distribution of adsorption sites. To evaluate the transport and concentration profiles of adsorbate in the pore, c_p (μmol/L), and the adsorbent loading, q_p (μmol/g), in a spherical particle of porous adsorbent, the following mass balance equation can be set up

$$\rho_p \frac{\partial q_p}{\partial t} + \varepsilon_p \frac{\partial c_p}{\partial t} = d_p \left(\frac{\partial^2 c_p}{\partial r^2} + \frac{2}{r} \frac{\partial c_p}{\partial r} \right) \quad (1)$$

where ρ_p is the activated carbon apparent density (g/L), t is time (s), ε_p is the AC porosity (dimensionless), d_p is the pore diffusion coefficient (m^2/s) and r is the radius of the adsorbent particle (m). The fitting parameter in the model was d_p. All other parameters were either calculated, measured or obtained from the AC supplier. AC porosity was calculated based on the ratio between the material apparent density and skeleton density. Details are given in the Supplementary Information (SI) 1. The particle radius used was the arithmetic mean of the particle size range (3.75×10^{-4} m).

At each point in the pore of the granule we assume a local equilibrium between the OMP concentration in the pore liquid and the adsorbent loading. This equilibrium is described by the Langmuir equation (Langmuir, 1918) given by

$$q_p = \frac{q_m K_L c_p}{1 + K_L c_p} \quad (2)$$

where q_m is the maximum adsorption capacity of the adsorbent (μmol/g) and K_L is the Langmuir constant (L/μmol).

2.1. Two boundary conditions are defined

1) The micropollutant concentration in the bulk solution is equal to the concentration in the AC pores at the boundary with the solution ($r = r_p$). This condition is based on the assumption that transport limitation due to film diffusion can be neglected.

$$c_p = c_l \text{ for } r = r_p \quad (3)$$

2) In the center of the particle ($r = 0$) the flux is zero.

$$\frac{\partial c_p}{\partial r} = 0 \text{ for } r = 0. \quad (4)$$

In order to solve Equations (1)–(4), a mass balance was setup for the batch experiments. Details are given in SI (S1).

3. Materials and methods

3.1. Granular activated carbon

Two different types of GAC were used in the experiments: AcquaSorb™ K-CS from Jacobi® (CS), a coconut shell carbon thermally activated and C Gran from Norit® (CG), a wood based carbon chemically activated with phosphoric acid. Textural properties were measured with nitrogen adsorption-desorption isotherms at 77 K using a Micrometrics TriStar 3000, details are given in SI (S2). The ACs differ in micro and mesoporosity (Table 1). Micropores constitute almost the entire internal surface area of CS, whereas micropores represent around 68% of the CG internal surface area and the remaining fraction is formed by mesopores.

Granules were sieved to obtain particles with a diameter between 0.5 mm and 1 mm. After sieving, granules were washed with demineralized water for 1 h, dried and stored. Before the experiments, GAC was dried overnight at 105 °C, weighed and boiled in demineralized water to remove entrapped air.

3.2. Organic micropollutants

A mixture of 10 OMPs was used in this study: 1H-benzotriazole (BTA), desphenyl-chloridazon (DPC), diclofenac (DCF), guanylurea (GNR), hexamethylenetetramine (HMTA), iopamidol (IOP), iopromide (IOPR), melamine (MEL), metformin (MET) and pyrazole (PRZ). DPC was purchased from Santa Cruz Biotechnology and AKOS, IOP was purchased from Sigma Aldrich and AKOS, IOPR was purchased from Sigma Aldrich and Bayer, PYR was purchased from Merck and all other micropollutants were purchased from Sigma Aldrich. Table 2 shows their distribution coefficient (Log D_{ow}), molecular weight (MW), maximum projection area and minimal projection diameter. Log D_{ow} is related to the log K_{ow} and pK_a of a molecule as described by Equations (5) and (6) (De Ridder et al., 2010). For neutral molecules, log D_{ow} equals log K_{ow} This parameter is often used to indicate hydrophilicity of a molecule, as hydrophilic compounds are characterized by a log D_{ow} <3.5 (Lima et al., 2015).

$$\text{Acids}: \ \log D_{ow} = \log K_{ow} - \log\left(1 + 10^{(\text{pH}-\text{p}Ka)}\right) \quad (5)$$

$$\text{Bases}: \ \log D_{ow} = \log K_{ow} - \log\left(1 + 10^{(\text{p}Ka-\text{pH})}\right) \quad (6)$$

IOP and IOPR were the largest molecules in the study, followed by DCF, as indicated by their molecular weight and maximum projection area. At pH 7.5 GNR and MET are positively charged (Markiewicz et al., 2017), DCF is negatively charged (De Ridder et al., 2011) and the remaining OMPs are charge-neutral.

These micropollutants were selected due to their relevance for drinking water treatment. They have recently been found in surface and groundwater in Europe at concentrations that might impair drinking water production free of organic contaminants (Alotaibi et al., 2015; Buttiglieri et al., 2009; RIWA-Maas, 2016; Ruff et al., 2015).

3.3. Adsorption experiments

Adsorption isotherm experiments and kinetic experiments were performed by adding a known amount of GAC to a glass serum bottle containing a mixture of 10 OMPs and demineralized water buffered with 10 mM Na_2HPO_4 and 10 mM KH_2PO_4 at pH 7.5. All OMPs were present in similar molar concentrations. The bottles were closed with butyl rubber stoppers and wrapped in aluminium foil to prevent OMPs photodegradation. Experiments were conducted in duplicate, at 20 °C and bottles were mixed at 120 rpm in horizontal position in an orbital shaker. The sample volume subtracted from each bottle was 0.5 mL at every sampling point. Samples were centrifuged for 10 min at 10,000 rpm in order to remove GAC particles, diluted when necessary and stored at −20 °C before analyses.

3.3.1. Isotherm experiments

For isotherm experiments 10 different initial concentrations of micropollutants were used, ranging from 0.6 to 58 μM for CG or 1.0–120 μM for CS. The initial concentration used in the kinetic experiments were within this concentration range (section 3.3.2). GAC mass and total liquid volume were respectively 0.1 g and 100 mL for CG, and 0.05 g and 50 mL for CS. Equilibrium concentrations were measured at day 8 for CG and day 21 for CS, with the exception of diclofenac, which was measured at day 21 also for CG. AC load at equilibrium was calculated based on the mass balance shown in Equation 7

$$q_{eq} = \frac{(c_0 - c_{eq})*V}{m_A} \quad (7)$$

where q_{eq} is the AC load at equilibrium (μmol/g), c_0 is the initial adsorbate concentration (μmol/L), c_{eq} is the adsorbate concentration at equilibirum (μmol/L), V is the liquid volume (L) and m_A is the adsorbent mass (g).

The Langmuir model was used to fit the experimental data using a nonlinear-optimization method as suggested by Tran et al. (2017) starting from the linearized form of the model given by Equation 8

$$\frac{1}{q_{eq}} = \frac{1}{q_m K_L c_{eq}} + \frac{1}{q_m}. \quad (8)$$

3.3.2. Kinetic experiments

Kinetic experiments were performed with initial OMP concentrations ranging from 34.7 to 60.9 μM, 0.1 g of GAC and a total liquid volume of 100 mL. Samples were taken at time 0, 2 min, 10 min, 30 min, 1 h, 5 h and days 1, 2, 4, 6, 8, 14 and 21. The final volume subtracted from the bottle due to this sampling campaign corresponded to less than 7% of the total liquid volume.

3.4. Chemical analyses

Micropollutants were measured using liquid chromatography coupled to high-resolution accurate-mass mass spectrometry (LC-HRAM-MS). The LC consisted of a Ultimate 3000 coupled through a Hesi II electrospray source to a QExactive Orbitrap MS (Thermo Scientific, San Jose, CA, USA). Sample volumes of 50 μL were injected onto an Atlantis T3 column (100 mm × 3 mm, 3 μm). Micropollutants were separated using gradient elution with a flow of 0.3 mL/min. Solvents were (A): water/ammonium formate 2mM/formic acid 0.016% (v/v) and (B): methanol/ammonium formate 2 mM/formic acid 0.016% (v/v). All solvents used were UHPLC grade, purchased from Actu-All (The Netherlands). The gradient applied was: 0–2 min linearly increased to 45% B, 2–8 min linearly increased to 100% B, 8–14.5 min stable at 100% B, decreased in 0.5 min to 0% B and stable at this condition until 20 min. The column temperature was maintained at 40 °C. Micropollutants were detected in positive ionisation mode using electrospray. Three different full-scan windows were applied: 60–160 for pyrazole, 700–800 for iopamidol and iopromide and 60–900 for all other micropollutants. The following MS conditions were applied: spray voltage 3.5 kV, sheath and sweep gas flow rates 48 and 2

Table 1
Textural properties of the activated carbons used in this study.

	Activation method	Micropore surface area (m^2/g)	Mesopore surface area (m^2/g)	Micropore volume (cm^3/g)	Mesopore volume (cm^3/g)
CG	Chemical	711	334	0.32	0.43
CS	Steam	1248	48	0.51	0.04

Table 2
Log D_{ow}, molecular weight (MW), maximum projection area and minimal projection diameter of micropollutants.

Micropollutant	Log D_{ow} at pH 7.0[a]	MW (g/mol)	Maximum projection area (Å[b])[c]	Minimal projection diameter (Å)[c]
1H-benzotriazole	1.23[b]	119.13	41.23	7.04
Desphenyl-chloridazon	−0.78[c]	145.55	42.76	7.82
Diclofenac	1.37[d] to 3[e]	296.15	69.33	9.70
Guanylurea	−2.06[c]	102.10	38.38	6.40
Hexamethylenetetramine	0.36[c]	140.19	36.39	7.34
Iopamidol	−2.4[e]	777.09	131.62	14.14
Iopromide	−2.1[e]	791.12	129.57	14.38
Melamine	−2.0[c]	126.12	45.30	8.00
Metformin	−4 to −3.2[f]	129.17	43.96	7.50
Pyrazole	0.02	68.08	26.57	5.94

[a] For BTA and PRZ, values reported in literature refer to Log K_{ow}.
[b] Hart et al. (2004).
[c] Marvin Scketch (v.16.9.12.0, ChemAxon Ltd.).
[d] Huntscha et al. (2012).
[e] Margot et al. (2013).
[f] ACD/Labs (V11.02).

respectively, capillary temperature 256 °C, aux gas heater temperature 413 °C and resolution 70000. MS was calibrated for each series according to manufacturer protocol using a Pierce™ LTQ Velos ESI Positive Ion Calibration Solution (Thermo Scientific). Peak identification and quantification was done with Thermo Xcalibur (version 2.2) software.

4. Results and discussion

4.1. Adsorption isotherms

Adsorption isotherms were performed to study the affinity of the selected OMPs for both types of activated carbons. All micropollutants showed a higher affinity for CS (Fig. 1), as shown in Table 3 (higher K_L values), except for MET and GNR, which showed a higher affinity for CG (Fig. 2). The affinity of OMPs for CG followed the order: DCF > IOPR > BTA > IOP > GNR > DPC > MEL > MET > PRZ. Affinity of OMPs for CS followed the order DCF > IOPR > IOP > BTA > MEL > DPC > PRZ > GNR. K_L values for metformin with CS and hexamethylenetetramine with both GACs could not be calculated accurately because hardly any adsorption was observed.

The maximum adsorption capacity of CS for some micropollutants can be higher than the q_m obtained in our experiments, given that the OMP concentrations applied were too low to reach CS saturation. Nevertheless, together with K_L it is justified to use this parameter to describe the distribution of the OMPs between the adsorbed and dissolved phase in the concentration range used in the kinetic experiments.

No OMP adsorption to butyl rubber stoppers was observed in controls without activated carbon (data not shown).

The higher carbon loading of CS with OMPs is most likely due to the larger micropore surface area of CS (Table 1). Stronger adsorption occurs in the micropores (Lu and Sorial, 2004) due to stronger interactions between the adsorbate and the pore walls (Li et al., 2002). A higher adsorption onto microporous AC compared to micro/mesoporous AC has previously been observed by Masson et al. (2016). Pyrazole showed low affinity for CS and almost no adsorption onto CG (Fig. 3). The low removal with both ACs is most likely related to the small molecule size (MW only 68) in relation to the AC pore size, which reduces the strength of the interactions between the molecule and the pore walls.

GNR, HMTA and MET showed a low affinity for the tested ACs. This may be related to their non-cyclic structure, restricting possible interactions of these micropollutants with the adsorbate. HMTA has a globular structure which restricts the available molecule surface for interaction with the AC. MET and GNR showed poor removal with activated carbon, as reported before (Scheurer et al., 2012). These are the only two positively charged molecules in our study, and both showed a higher affinity for CG than for CS. This is likely due to electrostatic interactions between these molecules and CG. Points of zero charge (pH_{PZC}) values ranging between 3.5 and 4.2 have been reported for CG (Butkovskyi et al., 2018; Villacañas et al., 2006). On the other hand, thermally activated carbons produced from coconut shells, such as CS, have typically pH_{pzc} values > 9 (De Ridder et al., 2013; Dittmar et al., 2018; Largitte and Pasquier, 2016). Therefore, CG most likely has more negatively charged surface groups than CS at neutral pH. Higher adsorption of cationic compounds compared with neutral and anionic compounds onto chemically activated carbons was also observed by Alves et al. (2018).

All micropollutants studied are hydrophilic and no correlation between the degree of hydrophilicity (represented by log D_{ow}) and their affinity for the GACs (represented by K_L) was observed. An exception to this observation was DCF, which had the highest log D_{ow} and highest K_L. Poor or no correlation between log D_{ow} and affinity for GAC for hydrophilic compounds is in agreement with what has been previously reported (De Ridder et al., 2010; Kovalova et al., 2013; Nam et al., 2014). For hydrophilic compounds, relevant interactions between adsorbate and activated carbon surface include pi-pi interactions, hydrogen bonds (De Ridder et al., 2010) and electrostatic interactions (Margot et al., 2013). OMPs with aromatic rings (for instance BTA and DCF) can interact with the AC surface via pi-pi interactions. All OMPs from this study are capable of forming H-bonds with the functional groups of the AC and charged molecules (DCF, GNR and MET) are subject to electrostatic attraction or repulsion with charged groups from the AC surface.

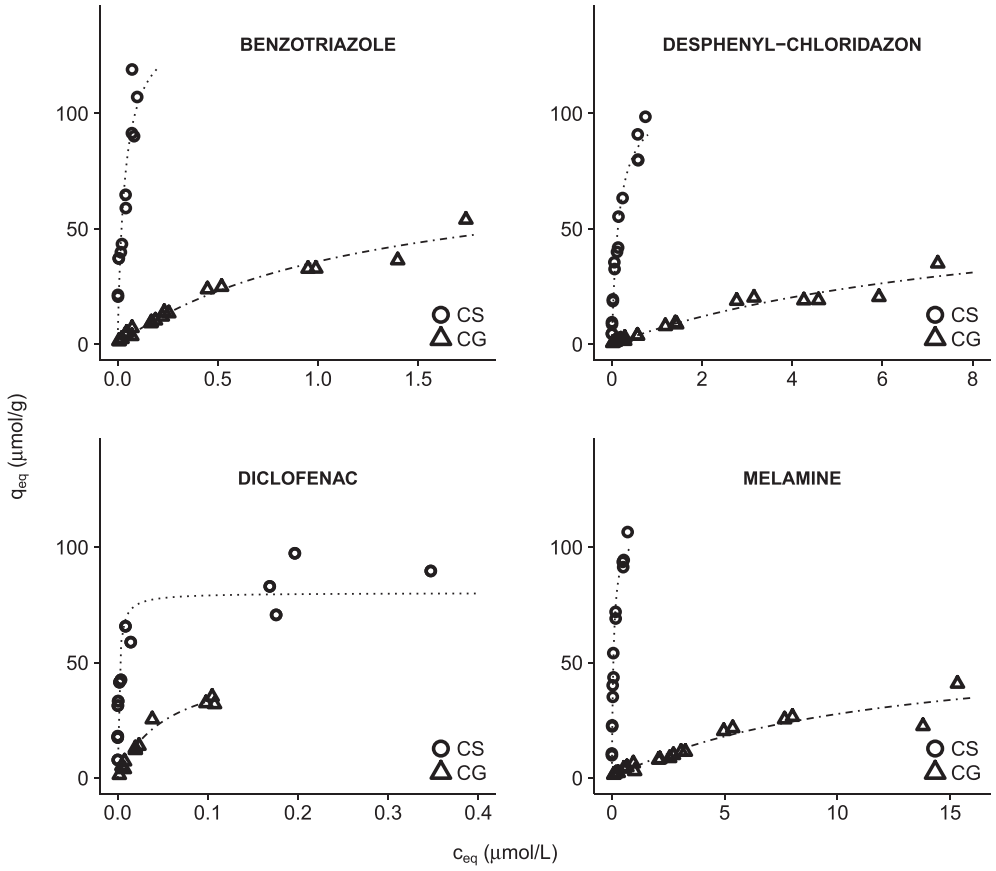

Fig. 1. Benzotriazole, desphenyl-chloridazon, diclofenac and melamine adsorption isotherms with CG and CS. Lines represent Langmuir model (Equation (2)).

Table 3
Langmuir coefficients of adsorption isotherms and correlation coefficient between experimental data and model prediction. NA: not available.

	CG			CS		
Micropollutant	K_L (L/µmol)	q_m (µmol/g)	R^2	K_L (L/µmol)	q_m (µmol/g)	R^2
BTA	0.79	80.94	0.97	27.75	141.17	0.87
DPC	0.11	66.00	0.94	6.45	108.41	0.97
DCF	18.17	51.43	0.98	685.44	80.25	0.88
GNR	0.19	87.87	0.97	0.01	202.15	0.94
IOP	0.74	78.56	0.91	37.83	69.42	0.89
IOPR	1.51	97.30	0.93	69.17	74.21	0.91
MEL	0.09	60.14	0.91	12.64	109.32	0.98
MET	0.06	95.07	0.96	NA	NA	NA
PRZ	1.2E-05	4E04	0.91	0.07	59.53	0.91

The high affinity of DCF and BTA for the ACs obtained in this experiment is in agreement with literature, as those micropollutants are often reported as highly adsorbable on activated carbon (Zietzschmann et al., 2016, 2014). The Langmuir affinity constant of DCF with both ACs was at least tenfold higher than for the other micropollutants. High affinity of DCF for the ACs may be related to the higher log D_{ow} of DCF compared to the other micropollutants studied (Table 2) and to the presence of two aromatic rings in the molecule, increasing the possibilities of pi-pi interactions (Bäuerlein et al., 2012).

IOP and IOPR showed a relatively high affinity for both ACs in our experiments, whereas these micropollutants are often reported as weakly adsorbable (Kennedy et al., 2015; Margot et al., 2013; Rossner et al., 2009; Zietzschmann et al., 2014). The divergence between our results and what is often reported in literature for IOP and IOPR can be explained by the absence of background organic matter in our experiments. The presence of dissolved organic carbon in concentrations as low as 1.5 mg/L can reduce the adsorption of IOP to GAC by a factor of 7 compared to the adsorption in demineralized water (Ahn et al., 2015). Due to the large size of these micropollutants, their removal with AC is more affected by the presence of background organic matter compared with the smaller compounds (Zietzschmann et al., 2015), either due to pore blockage or competition for adsorption sites. The difference between CG and CS load (q_{eq}) for IOP and IOPR is smaller than for the other micropollutants (Fig. 4). This indicates that not all micropore surface area of CS can be occupied by these molecules due to their large size, as predicted based on the molecules diameter (Table 2).

Possible interactions between the adsorbates in the mixture have not been taken into account when fitting the Langmuir as well as the Pore Diffusion models to our experimental data. We believe this approach can be justified, because based on the projected area

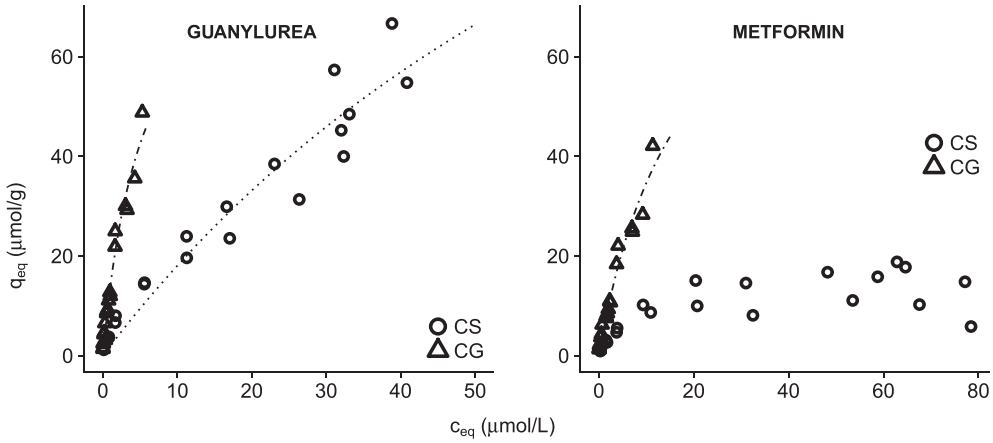

Fig. 2. Guanylurea and metformin adsorption isotherms with CG and CS. Lines represent Langmuir model (Equation (2)).

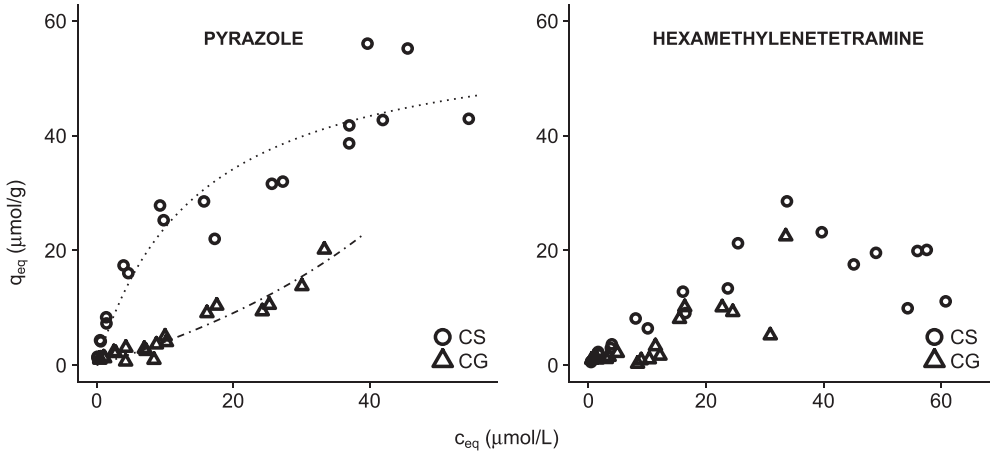

Fig. 3. Pyrazole and hexamethylenetetramine adsorption isotherms with CG and CS. Lines represent Langmuir model (Equation (2)).

of each compound (Table 2), at most only 15% of the GAC surface area available was used for adsorption. Moreover, displacement of an adsorbate with lower affinity for the AC by another adsorbate with higher affinity was less than 8% in the kinetic experiments (at $t > 120$ h), except for the pair guanylurea-CS in one of the replicates (18% decrease in adsorbed amount between day 8 and day 21). Therefore we conclude that mixtures of OMPs can be used to determine parameters for single solute isotherm and kinetic models.

4.2. Adsorption kinetics of OMPs onto GAC

In the kinetic adsorption studies, the adsorption rate was related to OMP molecular size and GAC pore size. We observed that equilibrium was reached within 24 h for the small molecules (BTA, DPC, GNR, MEL, MET, PRZ), whereas for DCF, equilibrium was reached within 24 h for CG and within 120 h for CS. For IOP and IOPR, the largest molecules in the study, equilibrium was reached within 50 h for CG and 300 h for CS.

Pore diffusion coefficients (d_p) were obtained by fitting the Pore Diffusion model to the kinetic data for the OMP-GAC pairs (Table 4). The obtained values of d_p are in the same range as previously reported for adsorption with activated carbon (Lesage et al., 2010; Ocampo-Pérez et al., 2012a). The value for d_p was not calculated for PRZ with CG since almost no adsorption was observed nor for MET with CS and HMTA with both ACs.

We observed a negative correlation between diffusion coefficients (d_p) and molecular size (Fig. S2), and a positive correlation between d_p and the presence of mesopores in GAC for BTA, DPC, DCF, IOP and IOPR. For these OMPs, the adsorption rate was higher for CG than CS (Fig. 5, Fig. S3 and Fig. S4), due to the presence of mesopores in CG (Table 1). For all micropollutants except for IOP and IOPR, the model curve was calculated using the average initial OMP concentration of the experimental duplicates. For IOP and IOPR with CG, the difference between the initial concentration of the duplicates was relatively high and thus two model curves were calculated using the initial concentrations of each duplicate.

Due to the faster adsorption of some OMPs onto CG than CS, CG load with those OMPs was higher than CS in the beginning of the adsorption process, despite the OMPs higher affinity for CS. The period during which CG load was higher than CS was proportional to the OMP molecular size: between 0.5 and 0.75 h for BTA and DPC, 12 h for DCF and between 25 and 73 h for IOP and IOPR. After this period, the CS load with OMPs was higher than CG, as expected based on affinity parameters. This is consistent with the hypothesis that the adsorption rate is limited by intra-particle diffusion and that mesopores facilitate the adsorbate diffusion into the granule (Valderrama et al., 2008). This was also observed by Masson et al. (2016) with activated carbon cloths with different mesopore volumes. Mesoporous ACs have been reported to be more suitable for adsorption of bulky molecules (Liu et al., 2006; Nakagawa et al., 2004; Yuan et al., 2007) compared to microporous ACs, due to

size exclusion. The overall affinity of the largest molecules tested (DCF, IOP and IOPR) is higher for CS than for CG. However, as discussed earlier, size exclusion effects of IOP and IOPR with CS can be observed in the isotherms, supporting the hypothesis that diffusion of these micropollutants in the micropores was hindered.

Some OMPs (GNR, MEL, MET and PRZ) showed no correlation between d_p and molecule size. PRZ is the smallest molecule in this study, but did not have the highest diffusion coefficient as could be expected based on its molecular weight. Moreover, GNR adsorbed at similar rates onto both ACs whereas MEL adsorbed faster onto CS (Fig. 6) indicating that the presence of mesopores in CG did not result in a faster adsorption rate of GNR and MEL onto this AC. No correlation between diffusion coefficient and affinity for the AC (represented by K_L) was observed either.

The lack of correlation between d_p and molecule size or affinity for the AC shows that properties of the OMP and/or GAC other than pore size also influence diffusion rates, such as AC chemical surface groups, OMP molecular shape, speciation, etc. In this study, it is not possible to distinguish the influence of mesopores from the effect of adsorbent surface chemistry because the used ACs differ in both aspects. A similar conclusion was obtained by Ocampo-Pérez et al. (2012a). In their study, no clear trend was obtained when comparing adsorption rates (given by second-order kinetics model) of compounds with different sizes onto GACs with different porosities.

The model describes the adsorption process after 0.5 h for the smaller molecules and after 24 h for the larger molecules. For early stages, the model overestimates the adsorbed amount of OMP. This may indicate that film-diffusion limits adsorption rate at the beginning of the adsorption process. Intra-particle diffusion is less relevant at initial stages since adsorption starts at the outer layers of the AC granules. This has been described by Valderrama et al. (2008) for polycyclic aromatic compounds and activated carbon. In their study with PAHs, the initial steps of the adsorption process could not be represented by models considering intra-particle diffusion as rate limiting step, due to the small thickness of the reacted layer. Our study shows that this is also valid for smaller polar molecules.

4.3. Pore diffusion coefficient

The pore diffusion coefficient of an adsorbate in AC is related to the adsorbate aqueous diffusion coefficient (D) as described by Equation (9) (Valderrama et al., 2008)

Table 4
Fitted pore diffusion coefficient (d_p) of OMPs in the two GACs, OMPs molecular weight (MW) and molecular diffusivities (D) based on Equation (10) and GAC tortuosity (τ) values based on Equation (9). NA: not available.

	d_p(m^2/s)		D (m^2/s)	MW (g/mol)	τ	
Micropollutant	CG	CS	–	–	CG	CS
BTA	$5.5{*}10^{-10}$	$3.5{*}10^{-10}$	$1.1{*}10^{-9}$	119.13	1.8	2.5
DPC	$3.5{*}10^{-10}$	$3.0{*}10^{-10}$	$1.2{*}10^{-9}$	145.55	3.0	3.1
DCF	$1.0{*}10^{-10}$	$6.0{*}10^{-11}$	$6.8{*}10^{-10}$	296.15	6.0	8.8
GNR	$3.0{*}10^{-10}$	$3.0{*}10^{-10}$	$1.5{*}10^{-9}$	103.00	4.4	3.8
HMTA	NA	NA	NA	140.19	NA	NA
IOP	$4.0{*}10^{-11}$	$2.0{*}10^{-11}$	$5.0{*}10^{-10}$	777.09	11.2	19.5
IOPR	$5.5{*}10^{-11}$	$2.5{*}10^{-11}$	$4.8{*}10^{-10}$	791.11	7.8	15.0
MEL	$1.5{*}10^{-10}$	$3.0{*}10^{-10}$	$1.2{*}10^{-9}$	126.12	7.3	3.2
MET	$1.5{*}10^{-10}$	NA	$1.0{*}10^{-9}$	129.17	6.2	NA
PRZ	NA	$1.5{*}10^{-10}$	$1.4{*}10^{-9}$	68.08	NA	7.3

$$d_p = \frac{D\varepsilon_p}{\tau} \tag{9}$$

where D is the molecular diffusivity of the adsorbate (m^2/s) and τ is the AC tortuosity factor (dimensionless), which is a parameter that describes the structure of AC and is used to relate the adsorbate diffusivity in the pore to the diffusivity in free solution.

D values for diclofenac and metformin have been reported in literature as $8.1{*}10^{-10}$ m^2/s (Cid-Cerón et al., 2016) and $1.23 * 10^{-9}$ m^2/s (Mondal et al., 2018), respectively. CS and CG tortuosity were calculated based on the reported D values and Equation (9). Tortuosity values calculated for CG are around 7, and the value for CS based on DCF is around 10, which are higher than tipically reported values in literature for AC (Ocampo-Pérez et al., 2012a; Worch, 2012).

When D values obtained experimentally are not available, empirical correlations are applied to calculate the molecular diffusivities. One of the most commonly used correlations is described by Wilke and Chang (Valderrama et al., 2008; Wilke and Chang, 1955; Worch, 2012) according to Equation 10

$$D = \frac{7.4{*}10^{-8}(\Phi M)^{0.5}T}{\eta_b V_A^{0.6}} \tag{10}$$

where Φ is an association parameter that represents the effective molecular weight of water with respect to the diffusion process, and has the value of 2.6, M is the solvent molecular weight (g/mol),

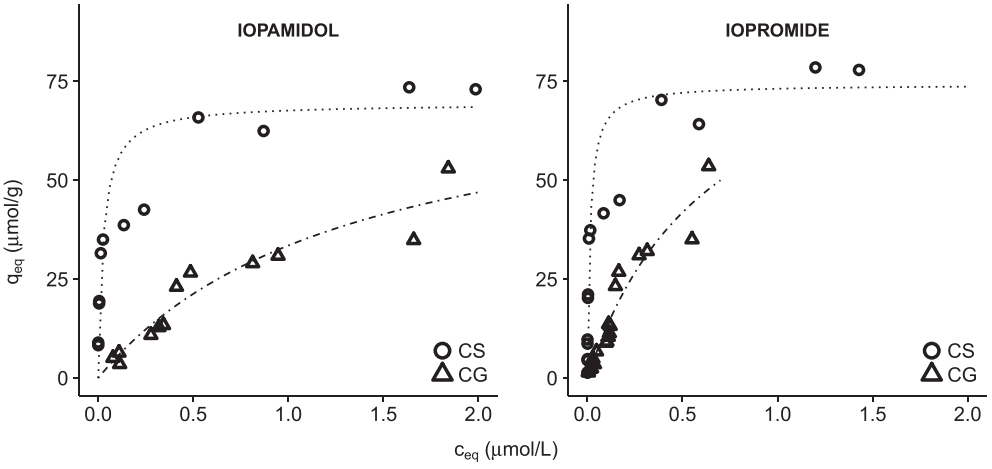

Fig. 4. Iopamidol and iopromide adsorption isotherms with CG and CS. Lines represent Langmuir model (Equation (2)).

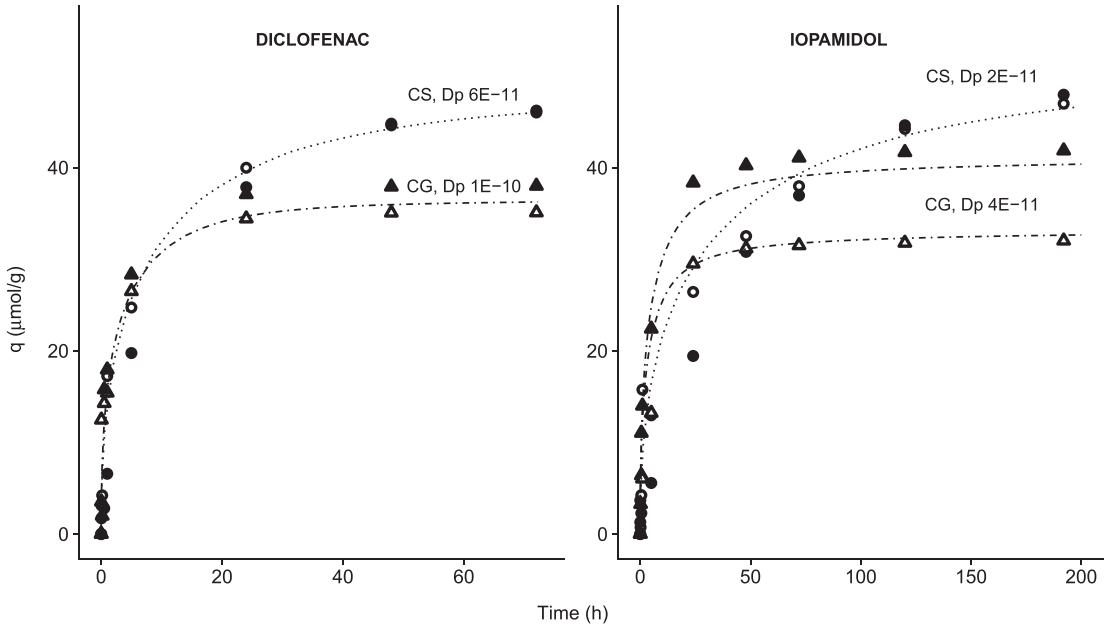

Fig. 5. Diclofenac and iopamidol AC load (q) in kinetic experiments. Experimental data and fitted pore diffusion model. Hollow and filled symbols represent duplicate batches. For iopamidol on CG, the two lines correspond to the model output with different initial concentrations.

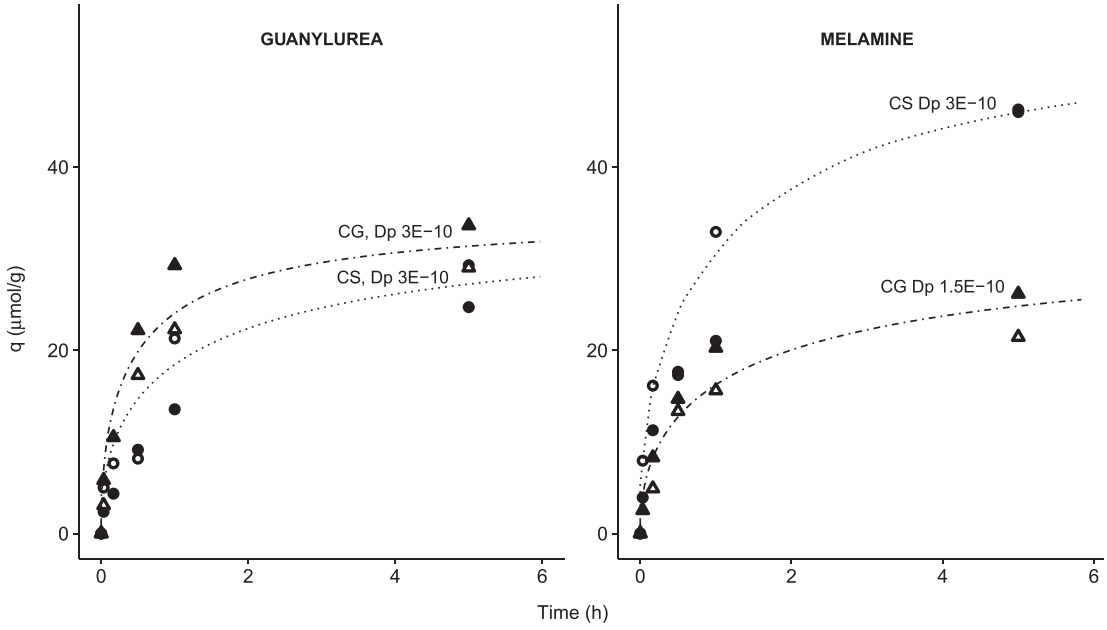

Fig. 6. Guanylurea and melamine AC load (q) in kinetic experiments. Experimental data and fitted pore diffusion model. Hollow and filled symbols represent duplicate batches.

T is temperature (K), η_b is the solution viscosity (cp) and V_A is the adsorbate molecular volume (cm^3/mol). Values for V_A for the OMPs were obtained by ChemSketch (ACD Labs) freeware.

Tortuosity values calculated using the aqueous diffusion obtained with Equation (10) are presented in Table 4. The calculated values are mostly in the range of values reported for AC except for MET and PRZ and the largest molecules DCF, IOP and IOPR. The high tortuosity value obtained for DCF, IOP and IOPR, combined with the adsorption kinetic results, indicates that their diffusion is hindered in the micropores, mainly in the GAC CS, likely due to the relatively large size of the molecules.

Since tortuosity is a property of AC, its values should be constant. However, this parameter is determined based on the adsorption of an adsorbate onto the AC surface, so the interaction between the adsorbate and the AC surface will likely influence the values obtained using experimental data. The variation in tortuosity values can also indicate that the intra-particle diffusion is not only governed by pore diffusion, but surface diffusion might also play a role in determining the adsorption rate. However, since CG and CS tortuosity and pore diffusion coefficients for the OMPs are not known, it is not possible to determine the relative contribution of surface diffusion to the adsorption rate.

5. Conclusions

The adsorption rate and affinity of OMPs with two types of activated carbons with different pore sizes was studied to determine the rate limiting step in adsorption. The main findings are as follows:

- The choice for the most suitable GAC for micropollutant removal from drinking water should take into account not only affinity for the target compounds but also GAC pore sizes. GACs with mesopores are desirable to prevent that slow kinetics reduce efficiency of a fixed-bed AC filter.
- Pore diffusion coefficients correlate negatively to adsorbate size for most OMPs and this correlation is stronger for the largest adsorbates.
- Neither molecule size nor adsorption affinity are sufficient to explain the adsorption kinetics of GNL, MER, MET, PRZ.
- Diffusion of the largest molecules is hindered in the GAC micropores, resulting in tortuosity values higher than typically reported for AC.
- Micropore surface area correlates with adsorption affinity between OMP and GAC. However, size-exclusion effects were observed for the largest OMPs iopamidol and iopromide.
- Log D_{ow} is a poor indicator for adsorption affinity for the hydrophilic OMPs studied.
- Adsorption affinity relates to OMP molecular structure: OMPs with cyclic structures adsorb to AC to a larger extent than OMPs with linear or globular structures.

Declaration of interests

The authors declare that they have no known competing financial interests or personal relationships that could have appeared to influence the work reported in this paper.

The authors declare the following financial interests/personal relationships which may be considered as potential competing interests:

Acknowledgement

This work was financially supported by Evides Water Company N.V. (Rotterdam, The Netherlands). We also want to thank David de Ridder for his valuable contribution to the discussion of the results, Tomas Haasterecht (Biobased Chemistry and Technology, Wageningen UR) for performing the nitrogen physiosorption analysis and helping with data interpretation, Jordi van Mook for his contribution to the experimental work when working at Evides Water Company N.V., and Marta Wells (Chemistry department, Tennessee Tech University) for providing values of Log D_{OW} data for metformin.

Appendix A. Supplementary data

Supplementary data to this article can be found online at https://doi.org/10.1016/j.watres.2019.06.012.

References

Ahn, Y., Cho, D., Kabra, A.N., Ji, M., Yoon, Y., 2015. Removal of Iopromide and its Intermediates from Ozone-Treated Water Using Granular Activated Carbon. https://doi.org/10.1007/s11270-015-2594-0.

Alotaibi, M.D., McKinley, A.J., Patterson, B.M., Reeder, A.Y., 2015. Benzotriazoles in the aquatic environment: a review of their occurrence, toxicity, degradation and analysis. Water. Air. Soil Pollut. 226, 225. https://doi.org/10.1007/s11270-015-2469-4.

Alves, T.C., Cabrera-Codony, A., Barceló, D., Rodriguez-Mozaz, S., Pinheiro, A., Gonzalez-Olmos, R., 2018. Influencing factors on the removal of pharmaceuticals from water with micro-grain activated carbon. Water Res. 144, 402–412. https://doi.org/10.1016/j.watres.2018.07.037.

Bäuerlein, P.S., Mansell, J.E., Ter Laak, T.L., De Voogt, P., 2012. Sorption behavior of charged and neutral polar organic compounds on solid phase extraction materials: which functional group governs sorption? Environ. Sci. Technol. 46, 954–961. https://doi.org/10.1021/es203404x.

Blanchard, G., Maunaye, M., Martin, G., 1984. Removal of heavy metals from waters by means of natural zeolites. Water Res. 18, 1501–1507. https://doi.org/10.1016/0043-1354(84)90124-6.

Butkovskyi, A., Sevenou, L., Meulepas, R.J.W., Hernandez Leal, L., Zeeman, G., Rijnaarts, H.H.M., 2018. Micropollutant removal from black water and grey water sludge in a UASB-GAC reactor. Water Sci. Technol. 77, 1137–1148. https://doi.org/10.2166/wst.2017.640.

Buttiglieri, G., Peschka, M., Frömel, T., Müller, J., Malpei, F., Seel, P., Knepper, T.P., 2009. Environmental occurrence and degradation of the herbicide n-chloridazon. Water Res. 43, 2865–2873. https://doi.org/10.1016/j.watres.2009.03.035.

Christoffels, E., Brunsch, A., Wunderlich-Pfeiffer, J., Mertens, F.M., 2016. Monitoring micropollutants in the Swist river basin. Water Sci. Technol. 74, 2280–2296. https://doi.org/10.2166/wst.2016.392.

Cid-Cerón, M.M., Guzmán-Hernández, D.S., Ramírez-Silva, M.T., Galano, A., Romero-Romo, M., Palomar-Pardavé, M., 2016. New Insights on the kinetics and mechanism of the electrochemical oxidation of diclofenac in neutral aqueous medium. Electrochim. Acta 199, 92–98. https://doi.org/10.1016/j.electacta.2016.03.094.

De Ridder, D.J., Verliefde, A.R.D., Heijman, S.G.J., Verberk, J.Q.J.C., Rietveld, L.C., Van Der Aa, L.T.J., Amy, G.L., Van Dijk, J.C., 2011. Influence of natural organic matter on equilibrium adsorption of neutral and charged pharmaceuticals onto activated carbon. Water Sci. Technol. 63, 416–423. https://doi.org/10.2166/wst.2011.237.

De Ridder, D.J., Verliefde, A.R.D., Schoutteten, K., Van Der Linden, B., Heijman, S.G.J., Beurroies, I., Denoyel, R., Amy, G.L., Van Dijk, J.C., 2013. Relation between interfacial energy and adsorption of organic micropollutants onto activated carbon. Carbon N. Y. 53, 153–160. https://doi.org/10.1016/j.carbon.2012.10.042.

De Ridder, D.J., Villacorte, L., Verliefde, A.R.D., Verberk, J.Q.J.C., Heijman, S.G.J., Amy, G.L., van Dijk, J.C., 2010. Modeling equilibrium adsorption of organic micropollutants onto activated carbon. Water Res. 44, 3077–3086. https://doi.org/10.1016/j.watres.2010.02.034.

Dittmar, S., Zietzschmann, F., Mai, M., Worch, E., Jekel, M., Ruhl, A.S., 2018. Simulating effluent organic matter competition in micro-pollutant adsorption onto activated carbon using a surrogate competitor. Environ. Sci. Technol. https://doi.org/10.1021/acs.est.8b01503.

Gunten, U. von, 2018. Oxidation processes in water treatment: are we on track? Environ. Sci. Technol. 52, 5062–5075. https://doi.org/10.1021/acs.est.8b00586.

Hart, D.S., Davis, L.C., Erickson, L.E., Callender, T.M., 2004. Sorption and partitioning parameters of benzotriazole compounds. Microchem. J. 77, 9–17. https://doi.org/10.1016/j.microc.2003.08.005.

Ho, Y.S., McKay, G., 1998. Kinetic models for the sorption of dye from aqueous solution by wood. Process Saf. Environ. Protect. 76, 183–191. https://doi.org/10.1205/095758298529326.

Hung, H., Lin, T., 2006. Adsorption of MTBE from contaminated water by carbonaceous resins and mordenite zeolite. J. Hazard Mater. 135, 210–217. https://doi.org/10.1016/j.jhazmat.2005.11.050.

Huntscha, S., Singer, H.P., McArdell, C.S., Frank, C.E., Hollender, J., 2012. Multiresidue analysis of 88 polar organic micropollutants in ground, surface and wastewater using online mixed-bed multilayer solid-phase extraction coupled to high performance liquid chromatography-tandem mass spectrometry. J. Chromatogr. A 1268, 74–83. https://doi.org/10.1016/j.chroma.2012.10.032.

Katsigiannis, A., Noutsopoulos, C., Mantziaras, J., Gioldasi, M., 2015. Removal of emerging pollutants through granular activated carbon. Chem. Eng. J. 280, 49–57. https://doi.org/10.1016/j.cej.2015.05.109.

Kennedy, A.M., Reinert, A.M., Knappe, D.R.U., Ferrer, I., Summers, R.S., 2015. Full- and pilot-scale GAC adsorption of organic micropollutants. Water Res. 68, 238–248. https://doi.org/10.1016/j.watres.2014.10.010.

Kovalova, L., Knappe, D.R.U., Lehnberg, K., Kazner, C., Hollender, J., 2013. Removal of highly polar micropollutants from wastewater by powdered activated carbon. Environ. Sci. Pollut. Res. 20, 3607–3615. https://doi.org/10.1007/s11356-012-1432-9.

Kyriakopoulos, G., Doulia, D., 2006. Adsorption of pesticides on carbonaceous and polymeric materials from aqueous solutions: a review. Separ. Purif. Rev. 35, 97–191. https://doi.org/10.1080/15422110600822733.

Langmuir, I., 1918. The adsorption of gases on plane surfaces of glass, mica and platinum. J. Am. Chem. Soc. 40, 1361–1403. https://doi.org/10.1021/ja02242a004.

Largitte, L., Pasquier, R., 2016. A review of the kinetics adsorption models and their application to the adsorption of lead by an activated carbon. Chem. Eng. Res. Des. 109, 495–504. https://doi.org/10.1016/j.cherd.2016.02.006.

Lee, V.K.C., Mckay, G., 2004. Comparison of solutions for the homogeneous surface diffusion model applied to adsorption systems. Chem. Eng. J. 98, 255–264. https://doi.org/10.1016/j.cej.2003.08.028.

Lesage, G., Sperandio, M., Tiruta-Barna, L., 2010. Analysis and modelling of non-equilibrium sorption of aromatic micro-pollutants on GAC with a multi-compartment dynamic model. Chem. Eng. J. 160, 457–465. https://doi.org/10.

1016/j.cej.2010.03.045.
Li, L., Quinlivan, P.A., Knappe, D.R.U., 2002. Effects of activated carbon surface chemistry and pore structure on the adsorption of organic contaminants from aqueous solution. Carbon N. Y. 40, 2085–2100. https://doi.org/10.1016/S0008-6223(02)00069-6.
Lima, L., Baêta, B.E.L., Lima, D.R.S., Afonso, R.J.C.F., Aquino, S.F. De, Libânio, M., 2015. Comparison between two forms of granular activated carbon for the removal of pharmaceuticals from different waters. Environ. Technol. 3330, 1–34. https://doi.org/10.1080/09593330.2015.1114030.
Liu, G., Zheng, S., Yin, D., Xu, Z., Fan, J., Jiang, F., 2006. Adsorption of aqueous alkylphenol ethoxylate surfactants by mesoporous carbon CMK-3. J. Colloid Interface Sci. 302, 47–53. https://doi.org/10.1016/j.jcis.2006.06.006.
Loos, R., Locoro, G., Comero, S., Contini, S., Schwesig, D., Werres, F., Balsaa, P., Gans, O., Weiss, S., Blaha, L., Bolchi, M., Gawlik, B.M., 2010. Pan-European survey on the occurrence of selected polar organic persistent pollutants in ground water. Water Res. 44, 4115–4126. https://doi.org/10.1016/j.watres.2010.05.032.
Lu, Q., Sorial, G.A., 2004. The role of adsorbent pore size distribution in multi-component adsorption on activated carbon. Carbon N. Y. 42, 3133–3142. https://doi.org/10.1016/j.carbon.2004.07.025.
Margot, J., Kienle, C., Magnet, A., Weil, M., Rossi, L., de Alencastro, L.F., Abegglen, C., Thonney, D., Chèvre, N., Schärer, M., Barry, D.A., 2013. Treatment of micro-pollutants in municipal wastewater: ozone or powdered activated carbon? Sci. Total Environ. 461–462, 480–498. https://doi.org/10.1016/j.scitotenv.2013.05.034.
Markiewicz, M., Jungnickel, C., Stolte, S., Białk-Bielińska, A., Kumirska, J., Mrozik, W., 2017. Ultimate biodegradability and ecotoxicity of orally administered antidiabetic drugs. J. Hazard Mater. 333, 154–161. https://doi.org/10.1016/j.jhazmat.2017.03.030.
Masson, S., Gineys, M., Delpeux-Ouldriane, S., Reinert, L., Guittonneau, S., Béguin, F., Duclaux, L., 2016. Single , binary , and mixture adsorption of nine organic contaminants onto a microporous and a microporous/mesoporous activated carbon cloth. Microporous Mesoporous Mater. 234, 24–34. https://doi.org/10.1016/j.micromeso.2016.07.001.
Miklos, D.B., Remy, C., Jekel, M., Linden, K.G., Drewes, J.E., Hübner, U., 2018. Evaluation of advanced oxidation processes for water and wastewater treatment – a critical review. Water Res. 139, 118–131. https://doi.org/10.1016/j.watres.2018.03.042.
Mondal, S., Samajdar, R.N., Mukherjee, S., Bhattacharyya, A.J., Bagchi, B., 2018. Unique features of metformin: a combined experimental, theoretical, and simulation study of its structure, dynamics, and interaction energetics with DNA grooves. J. Phys. Chem. B 122, 2227–2242. https://doi.org/10.1021/acs.jpcb.7b11928.
Nakagawa, K., Namba, A., Mukai, S.R., Tamon, H., Ariyadejwanich, P., Tanthapanichakoon, W., 2004. Adsorption of phenol and reactive dye from aqueous solution on activated carbons derived from solid wastes. Water Res. 38, 1791–1798. https://doi.org/10.1016/j.watres.2004.01.002.
Nam, S.-W., Choi, D.-J., Kim, S.-K., Her, N., Zoh, K.-D., 2014. Adsorption characteristics of selected hydrophilic and hydrophobic micropollutants in water using activated carbon. J. Hazard Mater. 270, 144–152. https://doi.org/10.1016/j.jhazmat.2014.01.037.
Nath, K., Bhakhar, M.S., 2011. Microbial regeneration of spent activated carbon dispersed with organic contaminants: mechanism, efficiency, and kinetic models. Environ. Sci. Pollut. Res. 18, 534–546. https://doi.org/10.1007/s11356-010-0426-8.
Nguyen, L.N., Hai, F.I., Kang, J., Price, W.E., Nghiem, L.D., 2012. Removal of trace organic contaminants by a membrane bioreactor-granular activated carbon (MBR-GAC) system. Bioresour. Technol. 113, 169–173. https://doi.org/10.1016/j.biortech.2011.10.051.
Ocampo-Pérez, R., Abdel daiem, M.M., Rivera-Utrilla, J., Méndez-Díaz, J.D., Sánchez-Polo, M., 2012a. Modeling adsorption rate of organic micropollutants present in landfill leachates onto granular activated carbon. J. Colloid Interface Sci. 385, 174–182. https://doi.org/10.1016/j.jcis.2012.07.004.
Ocampo-Perez, R., Leyva-Ramos, R., Alonso-Davila, P., Rivera-Utrilla, J., Sanchez-Polo, M., 2010. Modeling adsorption rate of pyridine onto granular activated carbon. Chem. Eng. J. 165, 133–141. https://doi.org/10.1016/j.cej.2010.09.002.
Ocampo-Perez, R., Leyva-Ramos, R., Mendoza-Barron, J., Guerrero-Coronado, R.M., 2011. Adsorption rate of phenol from aqueous solution onto organobentonite: surface diffusion and kinetic models. J. Colloid Interface Sci. 364, 195–204. https://doi.org/10.1016/j.jcis.2011.08.032.
Ocampo-Pérez, R., Leyva-Ramos, R., Rivera-Utrilla, J., Flores-Cano, J.V., Sánchez-Polo, M., 2015. Modeling adsorption rate of tetracyclines on activated carbons from aqueous phase. Chem. Eng. Res. Des. 104, 579–588. https://doi.org/10.1016/j.cherd.2015.09.011.
Ocampo-Pérez, R., Rivera-Utrilla, J., Gómez-Pacheco, C., Sánchez-Polo, M., López-Peñalver, J.J., 2012b. Kinetic study of tetracycline adsorption on sludge-derived adsorbents in aqueous phase. Chem. Eng. J. 213, 88–96. https://doi.org/10.1016/j.cej.2012.09.072.
Reemtsma, T., Berger, U., Arp, H.P.H., Gallard, H., Knepper, T.P., Neumann, M., Quintana, J.B., de Voogt, P., 2016a. Mind the gap: persistent and mobile organic compounds – water contaminants that slip through. Environ. Sci. Technol. acs.est.6b03338 https://doi.org/10.1021/acs.est.6b03338.
Reemtsma, T., Berger, U., Arp, H.P.H., Gallard, H., Knepper, T.P., Neumann, M., Quintana, J.B., Voogt, P. De, 2016b. Mind the gap: persistent and mobile organic compounds - water contaminants that slip through. Environ. Sci. Technol. 50, 10308–10315. https://doi.org/10.1021/acs.est.6b03338.
RIWA-Maas, 2016. Jaarrapport 2016 - De Maas 55.
Rossner, A., Snyder, S.A., Knappe, D.R.U., 2009. Removal of emerging contaminants of concern by alternative adsorbents. Water Res. 43, 3787–3796. https://doi.org/10.1016/j.watres.2009.06.009.
Ruff, M., Mueller, M.S., Loos, M., Singer, H.P., 2015. Quantitative target and systematic non-target analysis of polar organic micro-pollutants along the river Rhine using high-resolution mass- spectrometry e Identi fi cation of unknown sources and compounds. Water Res. 87, 145–154. https://doi.org/10.1016/j.watres.2015.09.017.
Scheurer, M., Michel, A., Brauch, H.-J., Ruck, W., Sacher, F., 2012. Occurrence and fate of the antidiabetic drug metformin and its metabolite guanylurea in the environment and during drinking water treatment. Water Res. 46, 4790–4802. https://doi.org/10.1016/j.watres.2012.06.019.
Scheurer, M., Sacher, F., Brauch, H.-J., 2009. Occurrence of the antidiabetic drug metformin in sewage and surface waters in Germany. J. Environ. Monit. 11, 1608–1613. https://doi.org/10.1039/b909311g.
Sjerps, R.M.A., Vughs, D., van Leerdam, J.A., ter Laak, T.L., van Wezel, A.P., 2016. Data-driven prioritization of chemicals for various water types using suspect screening LC-HRMS. Water Res. 93, 254–264. https://doi.org/10.1016/j.watres.2016.02.034.
Souza, P.R., Dotto, G.L., Salau, N.P.G., 2017. Detailed numerical solution of pore volume and surface diffusion model in adsorption systems. Chem. Eng. Res. Des. 122, 298–307. https://doi.org/10.1016/j.cherd.2017.04.021.
Stackelberg, P.E., Gibs, J., Furlong, E.T., Meyer, M.T., Zaugg, S.D., Lippincott, R.L., 2007. Efficiency of conventional drinking-water-treatment processes in removal of pharmaceuticals and other organic compounds. Sci. Total Environ. 377, 255–272. https://doi.org/10.1016/j.scitotenv.2007.01.095.
ter Laak, T.L., Kooij, P.J.F., Tolkamp, H., Hofman, J., 2014. Different compositions of pharmaceuticals in Dutch and Belgian rivers explained by consumption patterns and treatment efficiency. Environ. Sci. Pollut. Res. 21, 12843–12855. https://doi.org/10.1007/s11356-014-3233-9.
Ternes, T., 2007. The occurrence of micopollutants in the aquatic environment : a new challenge for water management. Water Sci. Technol. 327–332. https://doi.org/10.2166/wst.2007.428.
Ternes, T.A., Meisenheimer, M., McDowell, D., Sacher, F., Brauch, H.-J., Haist-Gulde, B., Preuss, G., Wilme, U., Zulei-Seibert, N., 2002. Removal of pharmaceuticals during drinking water treatment. Environ. Sci. Technol. 36, 3855–3863. https://doi.org/10.1021/es015757k.
Tran, H.N., You, S., Hosseini-bandegharaei, A., 2017. Mistakes and inconsistencies regarding adsorption of contaminants from aqueous solutions : a critical review. Water Res. 120, 88–116. https://doi.org/10.1016/j.watres.2017.04.014.
Valderrama, C., Gamisans, X., de las Heras, X., Farrán, A., Cortina, J.L., 2008. Sorption kinetics of polycyclic aromatic hydrocarbons removal using granular activated carbon: intraparticle diffusion coefficients. J. Hazard Mater. 157, 386–396. https://doi.org/10.1016/j.jhazmat.2007.12.119.
Villacañas, F., Pereira, M.F.R., Órfão, J.J.M., Figueiredo, J.L., 2006. Adsorption of simple aromatic compounds on activated carbons. J. Colloid Interface Sci. 293, 128–136. https://doi.org/10.1016/j.jcis.2005.06.032.
Wilke, C.R., Chang, P., 1955. Correlation of diffusion coefficients in dilute solutions. AIChE J. 1, 264–270.
Worch, E., 2012. Adsorption Technology in Water Treatment: Fundamentals, Processes, and Modeling. Walter de Gruyter GmbH & Co. KG, Berlin/Boston. https://doi.org/10.1515/9783110240238.
Yuan, X., Zhuo, S.-P., Xing, W., Cui, H.-Y., Dai, X.-D., Liu, X.-M., Yan, Z.-F., 2007. Aqueous dye adsorption on ordered mesoporous carbons. J. Colloid Interface Sci. 310, 83–89. https://doi.org/10.1016/j.jcis.2007.01.069.
Zhu, Q., Moggridge, G.D., Ainte, M., Mantle, M.D., Gladden, L.F., D'Agostino, C., 2016. Adsorption of pyridine from aqueous solutions by polymeric adsorbents MN 200 and MN 500. Part 2: kinetics and diffusion analysis. Chem. Eng. J. 306, 67–76. https://doi.org/10.1016/j.cej.2016.07.039.
Zietzschmann, F., Aschermann, G., Jekel, M., 2016. Comparing and modeling organic micro-pollutant adsorption onto powdered activated carbon in different drinking waters and WWTP effluents. Water Res. 102, 190–201. https://doi.org/10.1016/j.watres.2016.06.041.
Zietzschmann, F., Mitchell, R.-L., Jekel, M., 2015. Impacts of ozonation on the competition between organic micro-pollutants and effluent organic matter in powdered activated carbon adsorption. Water Res. 84, 153–160. https://doi.org/10.1016/j.watres.2015.07.031.
Zietzschmann, F., Worch, E., Altmann, J., Ruhl, A.S., Sperlich, A., Meinel, F., Jekel, M., 2014. Impact of EfOM size on competition in activated carbon adsorption of organic micro-pollutants from treated wastewater. Water Res. 65, 297–306. https://doi.org/10.1016/j.watres.2014.07.043.